MODEL-BASED SHAPE FROM CONTOUR AND POINT PATTERNS

by

Marijke F. Augusteijn
and
Charles R. Dyer

Computer Sciences Technical Report #542

May 1984

Model-based Shape from Contour and Point Patterns

Marijke F. Augustejn
Charles R. Dyer

Computer Sciences Department
University of Wisconsin
Madison, WI 53706

Abstract

A model-based approach is developed for recovering three-dimensional surface orientation from a single two-dimensional polygonal contour or point pattern. Two planar object models are analyzed -- rectangles and arbitrary point patterns. We define an iterative procedure which efficiently computes both the correspondence between model and image features (line segments) and the correct surface orientation.

1. Introduction

The recovery of three-dimensional shape and orientation from a single two-dimensional contour is a fundamental process in the human visual system. Recently a number of methods have been proposed for computing this same interpretation of surface orientation. For the most part these techniques have concentrated on identifying *general* constraints and assumptions about the nature of objects and the imaging geometry in order to recover a single "best" interpretation from among the many possible for a given image. For example, Kanade [1] defines shape constraints in terms of image space regularities such as parallel lines and skew symmetries. Witkin [2] looks for the most uniform distribution of tangents to a contour over a set of possible inverse projections in object space. Similarly, Brady and Yuille [3] search for the most compact shape (using the measure of area over perimeter squared) in the object space of inverse projected planar contours.

Rather than attempting to maximize some general shape-based evaluation function over the space of possible inverse projective transforms of a given image contour, we propose to more directly *match* a given model contour with the set of inverse projections. This model-based approach is important for three reasons. First, in many practical applications such as the robotics bin-picking problem and low-level aerial image understanding for navigation, there exist known models of the objects being viewed (e.g. an industrial part or an airport runway). Second, as Gregory has pointed out [4], human familiarity with many simple shapes such as circles and squares may be the basis for interpreting three-dimensional surface orientation. Finally, there exist many real world counterexamples to the non-purposive evaluation functions which have been developed to date. For example, Kanade's and Witkin's measures incorrectly estimate surface orientation for regular shapes such as ellipses (which are often interpreted as slanted circles). Brady's compactness measure does not correctly interpret non-compact figures such as rectangles since he will compute it to be a rotated square (e.g. if we view a rectangular table top we do not see it as a rotated square surface, but as a rotated rectangle).

Our general goal can be stated as follows. Given a model of an object contour and an image of that same contour from an unknown viewpoint, find the orientation of the contour with respect to the image plane which matches the given image. In this paper we will assume object models can be specified as either planar polygonal contours (defined as a list of line segments) or planar point sets. The imaging geometry assumes orthographic projection. While initially we will also assume that we know *a priori* the correspondence between the model line segments defining a contour and the observed image lines, we will drop this assumption later. Thus our solution incorporates finding both the correct correspondence between model and image features (line segments and points) and the correct surface orientation for each planar contour or point pattern.

2. The Geometric Model

We assume orthographic projection and use the geometric model used by Witkin [2]. Following his notation we assume an object plane S in space with an orthogonal coordinate system (x', y'). There is also an image plane I with coordinate system (x, y). The orientation of S with respect to I can be denoted by two angles σ and τ; the slant σ is the angle between I and S (which we will always take to be acute, i.e. $\sigma \in [0,\pi/2]$) and the tilt τ is the angle between the projection of the normal of S onto I and the x-axis in I ($\tau \in (-\pi/2,\pi/2]$).

Suppose there are two intersecting straight lines in the object plane S. Let their angles with the x'-axis be β_1 and β_2. We want to find the angles of their orthographic projections onto I with the x-axis. First let $\tau = 0$. Then the projection of S's normal is parallel to the x-axis, the y and y'-axes are both parallel to the line of intersection between I and S and the angle between the x and x'-axis is σ. Since in this case there will only be projective shortening in the x-direction by a factor $\cos\sigma$ it follows immediately that the relation between an angle β in S and an angle α^* in I is given by

$$\tan\alpha^* = \tan\beta \,/\, \cos\sigma. \tag{2.1}$$

To introduce tilt rotate the object plane around the z-axis (which is perpendicular to the image plane), keeping the slant constant. The projected normal (and the projected x'-axis) then rotates away from the x-axis over an angle τ. Since the projected line still makes an angle α^* with the projected normal it now follows that its angle α with the x-axis is given by $\alpha = \alpha^* + \tau$, or using (2.1), we obtain

$$\alpha = \tan^{-1}(\tan\beta \,/\, \cos\sigma) + \tau \tag{2.2}$$

as the relation between a line at angle β with the x'-axis in S and a line at angle α with the x-axis in I. Rewritten, we obtain the following as our geometric model of the imaging process:

$$\tan(\alpha-\tau) = \frac{\tan\beta}{\cos\sigma}. \tag{2.3}$$

If we are given an (orthographic) image of the two intersecting lines mentioned above then we can measure α_1 and α_2 with respect to an arbitrary x-axis in I. If it so happens that we also know the corresponding lines in S and their respective angles β_1 and β_2 with the x'-axis, then we can recover (σ, τ) of the object plane using the geometric model in the following way: Substitute (α_1, β_1) and (α_2, β_2) into Eq. (2.3). The result is two (nonlinear) equations in the unknowns σ, τ. Eliminate $\cos\sigma$ between them and introduce the abbreviation

$$C = \frac{\tan\beta_1}{\tan\beta_2} \quad \left(= \frac{\tan(\alpha_1-\tau)}{\tan(\alpha_2-\tau)} \right).$$

We then obtain the relation

$$\tan(\alpha_1-\tau) = C\,\tan(\alpha_2-\tau). \tag{2.4}$$

This equation could be solved analytically for τ resulting in a complicated expression. Alternatively, we use an iterative approach. We have chosen this method because it has interesting generalizations, as we will see below. Write Eq. (2.4) in one of two equivalent forms:

$$\tau = \alpha_1 - \tan^{-1}[C\tan(\alpha_2-\tau)], \tag{2.5}$$

$$\tau = \alpha_2 - \tan^{-1}[\frac{1}{C}\tan(\alpha_1-\tau)]. \tag{2.6}$$

These equations are now suitable for iteration as follows. Pick some initial value τ_0 and substitute it into the right hand side of either (2.5) or (2.6). Next, calculate its left hand side τ_1 and substitute

this "improved" value back into the right hand side of the selected equation, and so on. Thus, in iterative form, these equations become

$$\tau_{i+1} = \alpha_1 - \tan^{-1}[C \tan(\alpha_2 - \tau_i)], \quad i = 0,1,2,\ldots, \tag{2.7}$$

$$\tau_{i+1} = \alpha_2 - \tan^{-1}[\frac{1}{C}\tan(\alpha_1 - \tau_i)], \quad i = 0,1,2,\ldots. \tag{2.8}$$

These are no longer equivalent; they calculate τ-values in "reverse order", i.e. if $\tau_0, \tau_1, \ldots, \tau_{n-1}, \tau_n$ is a sequence that can be generated by (2.7) then $\tau_n, \tau_{n-1}, \ldots, \tau_1, \tau_0$ can be generated by (2.8). We will need to consider both forms. The iteration process should be continued until sufficient convergence is reached (or abandoned if no convergence is obtained).

3. Convergence of the Iteration Process

In this section we present graphical arguments to gain insight into the convergence of the iteration process. Consider Eq. (2.4). Fig. 1 shows the graphs of its left hand side and right hand side in the two cases $C<0$ (Fig. 1a) and $C>0$ (Fig. 1b). Intersections of these curves correspond to solutions of Eq. (2.4). First consider $C<0$. If the asymptotes of the two tangent functions coincide then there will only be one intersection in an interval of length π. But this implies $\alpha_1 = \alpha_2$, so that $\beta_1 = \beta_2$, which is inconsistent with $C<0$. Hence an interval $(\alpha_1 - \pi/2, \alpha_1 + \pi/2)$, over which $\tan(\alpha_1-\tau)$ is continuous is divided into two parts by an asymptote of $C\tan(\alpha_2-\tau)$. In the left interval $\tan(\alpha_1-\tau)$ and $C\tan(\alpha_2-\tau)$ cover the ranges $(-\infty, a]$ and $[b, -\infty)$ for some values a and b respectively. Since both are continuous there must be an intersection in this interval. A similar argument shows that there must also be an intersection in the right interval. Hence an interval of length π contains two intersections between the tangent curves, corresponding to two distinct solutions of Eq. (2.4).

Next consider $C>0$. Now no intersections need to exist, but then Eq. (2.4) has no solutions and this case is not of interest. As before, $\alpha_1 = \alpha_2$ is also uninteresting. Therefore assume the asymptotes again do not coincide. It is now easily shown that if there is one intersection between the curves, there must be a second one in a given interval of length π. As an example consider the case illustrated in Fig. 1b in which α_2 is to the right of α_1 and $0<C<1$. An intersection can only take place below the τ-axis. On the left of it $C\tan(\alpha_2-tau)$ is above $\tan(\alpha_1-\tau)$. A second intersection must exist because the asymptote of $C\tan(\alpha_2-\tau)$ is to the right of the asymptote of $\tan(\alpha_1-\tau)$. Similar arguments hold for the other three cases, when α_2 is to the left of α_1 with $0<C<1$, and when α_2 is to the left or right of α_1 with $C>1$. Hence, for any $C\neq 0$ for which the two curves intersect, Eq. (2.4) will have two generally distinct solutions; one of them will be the tilt τ we want to recover.

The iteration process can also be described graphically. We will illustrate this using Eq. (2.7). See Fig. 2. Pick some initial τ_0 and determine $y_0 = C\tan(\alpha_2-\tau_0)$ on the corresponding curve. Then move horizontally to the other curve, i.e. $y_0 = \tan(\alpha_1-\tau)$ and determine $\tau = \tau_1 = \alpha_1 - \tan^{-1}y_0$. Next move vertically to find $y_1 = C\tan(\alpha_2-\tau_1)$, and continue this process as shown. In this way we obtain a sequence $\tau_0, \tau_1, \tau_2, \ldots$. If $C<0$, as in Fig. 2a, then consecutive τ-values alternate being greater than and less than the solution point τ_s. The iteration thus forms a "spiral", which could be directed inward, toward the intersection, or outward away from it. On the other hand, when $C>0$ as in Fig. 2b, the entire sequence lies on one side of τ_s and the iteration forms a "staircase", which can either lead toward the intersection, or away from it. In either case in which the sequence is directed towards τ_s, it must converge unless it is possible for such a sequence to "turn around" and move away from this intersection point.

Consider an interval around τ_s that contains no asymptotes and assume that such a reversal is possible. Take a subsequence $\tau_i, \tau_{i+2}, \cdots$ in which all τ's correspond to points on the *same* tangent curve. In this case there exists some triple τ', τ'', τ''' such that $\tau'=\tau_j$, $\tau''=\tau_{j+2}$, and $\tau'''=\tau_{j+4}$ for some j, in which τ', τ'' is directed towards τ_s ($|\tau''-\tau_s| < |\tau'-\tau_s|$), but τ'', τ''' is directed away from τ_s ($|\tau'''-\tau_s| > |\tau''-\tau_s|$). Without loss of generality we can introduce a scaling factor such that $\tau_s=0$ and τ', τ'', τ''' are all positive (they are known to lie on the same side of τ_s). Then $\tau''<\tau'$ and $\tau''<\tau'''$. Now consider the first three elements of the iteration sequence, τ_0, τ_1 and τ_2. τ_1 and τ_2 are, of course, functions of the initial value τ_0. Because the tangent curves are monotonic and continuous on the given interval, it follows that the elements are continuous with respect to τ_0. Let τ_0 decrease continuously from τ' to τ''. Then τ_2 must increase continuously from τ'' to τ'''. Hence, there must exist a $\tau_k \in (\tau', \tau'')$ such that $\tau_0=\tau_2$. This implies that the sequence generated with initial value τ_k has the form $\tau_k, \tau_{k+1}, \tau_k, \tau_{k+1}, \cdots$ and is neither converging nor diverging. Graphically such a sequence corresponds to a rectangle.

We now derive the conditions for the existence of such an alternating sequence. Given an initial value τ_0 it follows from Eq. (2.7) that

$$\tau_1 = \alpha_1 - \tan^{-1}[C \tan(\alpha_2 - \tau_0)], \tag{3.1}$$

$$\tau_2 = \tau_0 = \alpha_1 - \tan^{-1}[C \tan(\alpha_2 - \tau_1)]. \tag{3.2}$$

Solving (3.2) for τ_1 we obtain

$$\tau_1 = \alpha_2 - \tan^{-1}[\frac{1}{C}\tan(\alpha_1 - \tau_0)]. \tag{3.3}$$

Eliminating τ_1 between (3.1) and (3.3) leads to an equation in τ_0:

$$\alpha_2 - \alpha_1 = \tan^{-1}[\frac{1}{C}\tan(\alpha_1 - \tau_0)] - \tan^{-1}[C \tan(\alpha_2 - \tau_0)]$$

$$= \tan^{-1}\left[\frac{\frac{1}{C}\tan(\alpha_1 - \tau_0) - C \tan(\alpha_2 - \tau_0)}{1 + \tan(\alpha_1 - \tau_0)\tan(\alpha_2 - \tau_0)}\right]. \tag{3.4}$$

Using the trigonometric identity

$$1 + \tan(\alpha_1 - \tau_0)\tan(\alpha_2 - \tau_0) = \frac{\tan(\alpha_2 - \tau_0) - \tan(\alpha_1 - \tau_0)}{\tan[(\alpha_2 - \tau_0) - (\alpha_1 - \tau_0)]}$$

we obtain

$$\tan(\alpha_2 - \alpha_1)[\tan(\alpha_2 - \tau_0) - \tan(\alpha_1 - \tau_0)] = \tan(\alpha_2 - \alpha_1)[\frac{1}{C}\tan(\alpha_1 - \tau_0) - C \tan(\alpha_2 - \tau_0)].$$

One solution of the equation is $\alpha_1 = \alpha_2$. But this implies $\beta_1 = \beta_2$ and we know that these two angles must be different. Another solution is $|\alpha_2 - \alpha_1| = \pi/2$. If we substitute this relation into Eq. (2.4) the resulting equation is easily solved and we find $\tau_s = \alpha_1 + \tan^{-1}\sqrt{-C}$ and $\tau_s = \alpha_1 - \tan^{-1}\sqrt{-C}$ as the two intersections in this case. Assuming that $|\alpha_2 - \alpha_1| = \pi/2$ does not hold $\tan(\alpha_2 - \alpha_1)$ can be canceled and the above equation becomes

$$\tan(\alpha_2 - \tau_0) - \tan(\alpha_1 - \tau_0) = \frac{1}{C}\tan(\alpha_1 - \tau_0) - C \tan(\alpha_2 - \tau_0). \tag{3.5}$$

Eq. (3.5) is an identity when $C = -1$. From the definition of C it follows that $\beta_1 = -\beta_2$ in this case. Also, Eq. (2.4) now takes the form: $\tan(\alpha_1 - \tau_s) = -\tan(\alpha_2 - \tau_s)$. Again this equation is easily solved and we obtain $\tau_s = (\alpha_1 + \alpha_2)/2$ and $\tau_s = (\alpha_1 + \alpha_2)/2 + \pi/2$ as the two intersection points. In both these cases, $|\alpha_2 - \alpha_1| = \pi/2$ and $\beta_1 = -\beta_2$, the iteration leads to a sequence $\tau_0, \tau_1, \tau_0, \tau_1, \cdots$ for *any* initial value τ_0. All spirals have degenerated into rectangles.

If $C \neq -1$ we can put Eq. (3.5) into the form

$$\frac{\tan(\alpha_1 - \tau_0)}{\tan(\alpha_2 - \tau_0)} = \frac{1+C}{1+1/C} = C. \tag{3.6}$$

But this is equivalent to Eq. (2.4), which we are trying to solve. If we happen to start the iteration from a solution τ_s we should expect all values in the sequence to be equal; the spiral or staircase has then contracted into a point.

Excluding the two exceptional cases it now follows that an iteration sequence entering the mentioned interval around an intersection point τ_s while approaching τ_s, must continue in this direction and converge to the solution $\tau = \tau_s$. Now recall that Eq. (2.7) and Eq. (2.8) generate τ-values in reverse order. Therefore, in such interval around an intersection either (2.7) or (2.8) converges to that intersection.

Empirically we have found that both iteration schemes (2.7) and (2.8) converge independent of initial value, each to a different solution. Also, it has been observed that, if $\tau_{s'}$ and $\tau_{s''}$ are the two

values satisfying (2.4), the relation

$$\frac{\tan(\alpha_i - \tau_{s'})}{\tan\beta_i} = \frac{\tan\beta_i}{\tan(\alpha_i - \tau_{s''})}, \quad i = 1,2 \tag{3.7}$$

holds between them. This is consistent with the relation

$$\frac{\tan(\alpha_1 - \tau_{s'})}{\tan(\alpha_2 - \tau_{s'})} \frac{\tan(\alpha_1 - \tau_{s''})}{\tan(\alpha_2 - \tau_{s''})} = C^2 = \frac{\tan^2\beta_1}{\tan^2\beta_2}$$

which can be derived from Eq. (2.4) for the solutions $\tau_{s'}$ and $\tau_{s''}$. Since $\tan\beta \,/\, \tan(\alpha - \tau_s) = \cos\sigma \leq 1$, it is easy to determine which of the two solutions corresponds to the correct tilt τ.

4. Shape from Rectangles

The main limitation in Section 2 is that in general we do not know the β-angles of lines with the x'-axis in the object plane S. Hence we can't determine the correct correspondence between the α's and β's. However, if the object plane is known to contain a rectangle with known ratio m between its sides, then we can calculate slant and tilt from the corresponding parallelogram in the image plane without knowing the corresponding β-angles explicitly. Referring to Fig. 3, let the angles between the rectangle's sides and the x'-axis be denoted by β_1 and β_2. Hence $\beta_1 - \beta_2 = \pi/2$. The angles between the diagonals and the x'-axis are β_3 and β_4. The relation between these angles is most easily seen if we introduce the auxiliary angle $\delta = \beta_3 - \beta_1$, so that $\tan\delta = m$, the ratio of the lengths of the rectangle's sides. The fourth angle can be written as $\beta_4 = \beta_1 - \delta$ and is *not* independent from the other three (but will be used for computational reasons below). Obviously, shape and orientation of the rectangle are completely determined by β_1, β_2 and β_3 (its absolute size can never be obtained from just angles).

We now use Eq. (2.3) for the four lines defining the rectangle with the following substitutions:

$$\tan\beta_2 = \tan(\beta_1 - \pi/2) = -1 / \tan\beta_1,$$

$$\tan\beta_3 = \tan(\beta_1 + \delta) = \frac{\tan\beta_1 + m}{1 - m\tan\beta_1},$$

$$\tan\beta_4 = \tan(\beta_1 - \delta) = \frac{\tan\beta_1 - m}{1 + m\tan\beta_1}.$$

Then the four equations become:

$$\tan(\alpha_1 - \tau) = \frac{1}{\cos\sigma}\tan\beta_1, \tag{4.1}$$

$$\tan(\alpha_2 - \tau) = -\frac{1}{\cos\sigma}\frac{1}{\tan\beta_1}, \tag{4.2}$$

$$\tan(\alpha_3 - \tau) = \frac{1}{\cos\sigma}\frac{\tan\beta_1 + m}{1 - m\tan\beta_1}, \tag{4.3}$$

$$\tan(\alpha_4 - \tau) = \frac{1}{\cos\sigma}\frac{\tan\beta_1 - m}{1 + m\tan\beta_1}. \tag{4.4}$$

It is easily derived from Eq. (4.1) and Eq. (4.2) that

$$\cos^2\sigma = [-\tan(\alpha_1 - \tau)\tan(\alpha_2 - \tau)]^{-1}, \tag{4.5}$$

$$\tan^2\beta_1 = -\tan(\alpha_1 - \tau) / \tan(\alpha_2 - \tau). \tag{4.6}$$

Multiplying Eq. (4.3) and Eq. (4.4) gives

$$\tan(\alpha_3 - \tau)\tan(\alpha_4 - \tau) = \frac{1}{\cos^2\sigma}\frac{\tan^2\beta_1 - m^2}{1 - m^2\tan^2\beta_1}.$$

If we now substitute Eq. (4.5) and Eq. (4.6) into this expression we arrive at an equation only in τ:

$$\tan(\alpha_3 - \tau)\tan(\alpha_4 - \tau) = \tan(\alpha_1 - \tau)\tan(\alpha_2 - \tau)\left[\frac{\tan(\alpha_1 - \tau) + m^2\tan(\alpha_2 - \tau)}{\tan(\alpha_2 - \tau) + m^2\tan(\alpha_1 - \tau)}\right]. \tag{4.7}$$

This can be written in iterative form:

$$\tau_{i+1} = \alpha_3 - \tan^{-1}\left[\frac{\tan(\alpha_1-\tau_i)\tan(\alpha_2-\tau_i)}{\tan(\alpha_4-\tau_i)}\;\frac{\tan(\alpha_1-\tau_i)+m^2\tan(\alpha_2-\tau_i)}{\tan(\alpha_2-\tau_i)+m^2\tan(\alpha_1-\tau_i)}\right]. \qquad (4.8)$$

The use of the dependent Eq. (4.4) is now clear -- without it the iteration equation would contain square roots. As τ varies through its sequence, arguments may become negative and we would have to consider imaginary angles. Note that if the rectangle happens to be a square, i.e., $m=1$, the second factor inside the brackets evaluates to 1 and a much simpler formula results.

Given an image plane with a parallelogram that is known to be the orthographic projection of a rectangle with known ratio of sides m, all we need to do is measure the angles α_1, α_2, α_3 and α_4 with respect to an arbitrary x-axis. Substituting these values into Eq. (4.8) we obtain the tilt τ of the object plane by means of the given iteration formula. Note that Eq. (4.7) is of the form of Eq. (2.4) with the constant C in (2.4) replaced by a function of τ. Thus, the iteration process too may be quite similar to the one studied in the previous section. Convergence of Eq. (4.8) is not garanteed, but the results of the previous section will still be helpful in analyzing its behavior.

We have observed that the two non-converging cases of the previous iteration, $|\alpha_2-\alpha_1|=\pi/2$ and $\beta_1=-\beta_2$ are also non-converging here. The first mentioned corresponds to a pure rotation, that is the slant is zero and no tilt can be defined. In the last mentioned case it follows that $|\beta_1|=\pi/4$, since $\beta_2-\beta_1=\pi/2$, hence $|\tan\beta_1|=1$. Substituting this value into Eq. (4.6) we obtain an equation that, changed into an iteration formula, was shown in the previous section not to converge but is easily solved directly. In all other cases we found that either Eq. (4.8) or a similar iterative formula, with α_3 and α_4 interchanged (that calculates a τ-sequence in reverse order), converges to a solution. Depending on the initial τ_0 value, the same formula was observed to converge to two distinct values that differ by $\pi/2$. It is easily verified that if τ_s satisfies Eq. (4.7) then $\tau_s + \pi/2$ will also satisfy this equation. The correct tilt can be determined by means of the criterion $-\tan(\alpha_1-\tau)\tan(\alpha_2-\tau) \geq 1$, which immediately follows from Eq. (4.5) and which can only be satisfied by one of these solutions Eq. (4.5) is then used to calculate the slant σ.

When modeling objects which consist of multiple planar faces, this method can be used to quantitatively recover the angles between the faces from their projected image planes. For two object planes separated at angle γ this angle can easily be determined from their normal directions $(p_1,q_1,1)$ and $(p_2,q_2,1)$ by means of

$$\cos\gamma = \frac{p_1p_2 + q_1q_2 + 1}{[(p_1^2 + q_1^2 + 1)(p_2^2 + q_2^2 + 1)]^{\frac{1}{2}}}. \qquad (4.9)$$

We need to express (p,q) in terms of (σ,τ). Since the angle between image plane and object plane is σ, the length of the projected normal follows as $\sqrt{p^2+q^2} = \tan\sigma$. Also, this projection makes an angle τ with the x-axis. Therefore, $(p,q) = (\tan\sigma\cos\tau, \tan\sigma\sin\tau)$. There is a complication in the sense that τ can only be determined from the geometric model modulo π and the assignment $(p,q) = (-\tan\sigma\cos\tau, -\tan\sigma\sin\tau)$ is also correct. This, of course, does not influence the direction of the projected normal, but if we try to restore the three-dimensional normal direction $(p,q,1)$ then the assignment of the sign makes a difference. This problem is of course inherent to orthographic projection, where information about the z-direction is lost.

However, it is possible to determine γ if we also use the properties of the gradient space (p,q). As is well known, if $G_1=(p_1, q_1)$ and $G_2=(p_2, q_2)$ correspond to two intersecting planes, then the line through G_1 and G_2 in gradient space is perpendicular to the edge between the corresponding planes in the image space. Using this fact we can find a consistent pairing (p_1, q_1) and (p_2, q_2). They both may have the wrong sign, but that does not affect Eq. (4.9). If the convexity of the edge is known, we can also determine the signs of (p_1, q_1) and (p_2, q_2).

4.1. Examples

4.1.1. A Cube

Suppose we are given an image of a cube as shown in Fig. 4. The three visible faces are labeled I, II, and III, and we will determine (σ, τ) for each of them. First, we measure the four α-angles for each face (Fig. 4 shows the set corresponding to face I). Next, the tilt for each face can be calculated by means of a simplified version of iteration formula (4.8) obtained by setting the ratio of the sides m equal to 1. After the tilt has been computed, we calculate the slant from Eq. (4.5) and these two angles are then used to determine the direction (p,q) of the projected normal to each face. The results are summarized in Table 1.

face	α_1	α_2	α_3	α_4	tilt τ	slant σ	(p, q)
I	9	69	39	-51	-51	54.7	(0.89, -1.10)
II	69	-51	-81	9	9	54.7	(1.39, 0.22)
III	9	-51	69	-21	69	54.7	(0.51, 1.32)

Table 1. The α-set, slant, tilt, and direction of the projected normal of each face of the cube in Fig. 4. All angles are expressed in degrees in the appropriate intervals.

In order to verify that the faces of the cube are indeed perpendicular, we need to substitute the (p,q) pairs with the appropriate signs into Eq. (4.9), i.e. we need to restore the three-dimensional normal direction $(p, q, 1)$. We will determine these signs by means of Fig. 5 in which (p, q) coordinates are superimposed on the (x, y) coordinates of the image. The gradients in Table 1 are denoted by the points G_I, G_{II} and G_{III} (with the indices corresponding to the faces); their counterparts with opposite signs are shown as G_I', G_{II}' and G_{III}'. To find the correct combinations, connect each G_i, $i = I, II, III$, either with G_j or with G_j' depending on which connecting line is perpendicular to the edge between the adjacent faces i and j. Two possible solutions are obtained -- one corresponds to a cube with convex edges and the other corresponds to a "cubical hole" with concave edges. Table 2 shows the corresponding $(p, q, 1)$ assignments in each case. It is now readily verified by means of Eq. (4.9) that each pair of faces belonging to the same set is indeed perpendicular.

face	$(p, q, 1)$ convex case	$(p, q, 1)$ concave case
I	(0.89, -1.10, 1)	(-0.89, 1.10, 1)
II	(-1.39, -0.22, 1)	(1.39, 0.22, 1)
III	(0.51, 1.32, 1)	(-0.51, -1.32, 1)

Table 2. The three faces of the cube and their three-dimensional gradients in the convex and concave cases.

4.1.2. A Paper-Folding

We consider an object consisting of a square piece of paper which is folded in the middle, forming two rectangles each with a ratio of its sides equal to 0.5. In orthographic projection one

view is shown in Fig. 6. We will calculate the angle between the two folds of paper from this image. The procedure is as before -- we measure the four α angles of each plane sheet in the image and calculate the tilt from Eq. (4.8) with $m = 0.5$. Then the slant follows from Eq. (4.5) and the gradient (p, q) is calculated from (σ, τ). The results are summarized in Table 3.

face	α_1	α_2	α_3	α_4	tilt τ	slant σ	(p, q)
I	-8.0	-56.0	13.4	-21.0	65.3	64.7	(0.88, 1.92)
II	-8.0	65.3	14.7	-37.3	-69.9	42.8	(0.40, -0.80)

Table 3. The α-set, slant, tilt, and gradient of the two faces of the paperfold in Fig. 6. All angles are expressed in degrees.

It is easily verified that the resulting gradients correspond to a line $G_I\ G_{II}$ in (p, q) space which is approximately perpendicular to the fold in (x, y) space (a small deviation is due to inaccuracy in the measurement of the α's). It now follows from Eq. (4.9) that the angle between the two normals is about 93 °, so the fold is approximately 87 °.

5. Shape from Arbitrary Point Patterns

In this section we derive how slant and tilt can be recovered from an image of a known point pattern in the object plane. The method can be applied to any planar pattern of points. In aerial image understanding applications such points may correspond to landmark points from a map database. In robotics applications these points might be corner features derived from a CAD database. In general, given any pattern of n points we will first translate it into a set of n angles and then apply our geometric model. In order to do this we need an origin and a direction of the x'-axis. A natural choice of origin is the centroid of the pattern. Suppose the points have coordinates (x_i', y_i'), $i=1,\ldots,n$, with respect to some coordinate system, then their centroid is given by

$$X' = \frac{1}{n}\sum_{i=1}^{n} x_i' \quad , \qquad Y' = \frac{1}{n}\sum_{i=1}^{n} y_i' \quad . \tag{5.1}$$

The orthographic projection is simplest when $\tau = 0$. Then x'-coordinates are shortened by a factor $\cos\sigma$ while y'-coordinates remain unchanged. It immediately follows from Eq. (5.1) that the centroid of the pattern in the object plane projects into the centroid of the projected pattern in the image plane. This remains true when $\tau \neq 0$ since a change in τ corresponds to a rotation of the entire pattern. Thus, we will use the centroid of each pattern as the origin in the corresponding plane.

The direction of the x'-axis in the object plane is always such that its projection and the projection of the normal direction of the object plane onto the image plane are parallel. So the x'-axis has a fixed direction, but this direction is not known. To remedy this problem we do the following. Connect all points in the object plane with their centroid. The angles between these connection lines are now computed. Select one of these lines and determine the angles between this one and all others; denote this set by $\beta_2, \beta_3, \ldots, \beta_n$. Now take the position of the x'-axis into account by adding an unknown angle ν to the entire set. Thus, the n points in the object plane correspond to n angles $\nu, \nu+\beta_2, \ldots, \nu+\beta_n$. The geometric model now takes the form:

$$\frac{\tan(\alpha_i - \tau)}{\tan(\beta_i + \nu)} = \frac{1}{\cos\sigma}, \quad i=1,\ldots,n, \tag{5.2}$$

with $\beta_1 = 0$, and contains the three unknowns σ, τ and ν. Obviously, the pattern must consist of at least three points in order to determine these unknowns. Since generally there will be many more than three points in the model pattern, we will base our equations on any four of them. As before the α's are known because they can be measured in the image with respect to some x-axis. At this point we will also assume that we know how to match the α's and β's. (We will remove this restriction later.) Then we can take the four selected pairs $(\alpha_1, \beta_1), \ldots, (\alpha_4, \beta_4)$ and substitute each of them into Eq (5.2). The result is four equations in which we can eliminate $\cos\sigma$ pairwise and obtain:

$$\frac{\tan(\alpha_1 - \tau)}{\tan(\beta_1 + \nu)} = \frac{\tan(\alpha_2 - \tau)}{\tan(\beta_2 + \nu)}, \tag{5.3}$$

$$\frac{\tan(\alpha_3 - \tau)}{\tan(\beta_3 + \nu)} = \frac{\tan(\alpha_4 - \tau)}{\tan(\beta_4 + \nu)}. \tag{5.4}$$

These equations cannot be solved explicitly for τ and ν, but note that they are similar to Eq. (2.4) if we replace C in that equation by a quotient of tangent functions. We will again try to find a solution by means of iteration. Since there are two unknowns that appear in both equations, the iteration formulas will be coupled and both ν and τ must converge simultaneously for the entire process to succeed.

Using Eq. (2.4) there were two iteration schemes and only one of them converged to the correct tilt. Here there are four pairs; for example, one of them is:

$$\tau_{i+1} = \alpha_1 - \tan^{-1}\left[\frac{\tan(\beta_1+\nu_i)}{\tan(\beta_2+\nu_i)}\tan(\alpha_2-\tau_i)\right], \tag{5.5}$$

$$\nu_{i+1} = -\beta_3 + \tan^{-1}\left[\frac{\tan(\alpha_3-\tau_{i+1})}{\tan(\alpha_4-\tau_{i+1})}\tan(\beta_4+\nu_i)\right], \quad i=0,1,2,.... \tag{5.6}$$

The other three are obtained by interchanging the (α, β) pairs in Eq. (5.5) but not in Eq. (5.6), or interchanging them in Eq. (5.6) but not in Eq. (5.5), or interchanging them in both equations. We do not know in advance which iteration schemes converge to the correct (τ, ν) and we may have to consider all four of them to find the solution. Convergence is not guaranteed. We have observed that no convergence occurs when a solution is close to an asymptote of one of the tangent functions. When $n>4$ choosing a different set $(\alpha_1, \beta_1), \ldots, (\alpha_4, \beta_4)$ can solve this problem. Empirically we have found that convergence was achieved in almost all cases using the first set of pairs selected. We did not encounter any special cases here, for which a lack of convergence could be predicted from the given set of angles. One of our experiments is described in Section 5.1.

If a pair (τ_s, ν_s) is a solution to Eq. (5.3) and Eq. (5.4), then the pair $(\tau_s+\pi/2, \nu_s+\pi/2)$ is also a solution, as immediately follows from these equations. It has been observed that the same iteration scheme converged to either (τ_s, ν_s) or $(\tau_s+\pi/2, \nu_s+\pi/2)$, depending on the initial value τ_0. Eq. (5.2) enables us to distinguish between these solutions because, in general, only one set also satisfies $\cos\sigma \leq 1$. However, an additional complication here is that the other three iteration schemes often converge to unwanted values.

Before discussing how the correct tilt can be distinguished from other candidate solution points that may result from the iteration, let us consider the more fundamental (but related) question of determining the correct match between a set of β-angles in the object plane and their projections, the α-angles in the image plane. Let us first study this projection in the simple case in which both τ and ν are zero. Then the relation

$$\tan\alpha_i = \frac{\tan\beta_i}{\cos\sigma}, \quad i=1,\ldots,n \tag{5.7}$$

holds between the two sets of angles. Excluding the trivial case when $\sigma=0$, it is seen that $|\tan\alpha_i| > |\tan\beta_i|$ and $|\alpha_i| > |\beta_i|$ since the tangent function is monotonically increasing on the interval $(-\pi/2, \pi/2)$. Fig. 7 illustrates the transformation. The set of α-angles tend to populate the region around the origin more thinly and the region near the asymptotes more densely than the set of β-angles. The "gap" around the origin and the "clustering" near the asymptotes will be more pronounced for larger slants. Reintroducing the angles ν and τ into the geometric model is equivalent to a shift in the entire set of β-angles and α-angles, respectively, and does not affect the properties of the transformation otherwise. It is evident from Eq. (5.7) and Fig. 7 that the transformation cannot change the ordering of the angles. That is, if both sets have increasing order on the interval $(-\pi/2, \pi/2]$ and the two angles β_k and α_l have been matched, then the entire correspondence is specified by the pairs (assuming addition modulo n): $(\alpha_{l+i}, \beta_{k+i})$, $i=0,\ldots,n-1$.

The correct correspondence is most easily determined when the slant is small. When $\cos\sigma \approx 1$ the difference between consecutive β-angles will be approximately preserved by the transformation and we match accordingly. When the slant is larger this will no longer be the case, but still the smallest difference between the β-angles will often be transformed into the smallest difference between the α-angles. We will pair the α's and β's using this heuristic to obtain our first candidate match. Next we choose any four pairs $(\alpha_1, \beta_1), \ldots, (\alpha_4, \beta_4)$ from the n possible and use these for our iteration schemes. If no convergence is reached at all, we assume that the match was incorrect and we form the next candidate match by assuming that the smallest difference between the β's is transformed into the next smallest difference between the α's. Otherwise, if convergence to (τ_s, ν_s) is obtained, we must verify the correctness of this solution. This is done using Eq. (5.2). From the candidate match (α_i, β_i) and the candidate solution (τ_s, ν_s) we compute the expressions

$\tan(\alpha_i - \tau_s)$ and $\tan(\beta_i + \nu_s)$ for each $i = 1,\ldots,n$. It follows from Eq. (5.2) that the correct match of angles and correct shifts ν, τ, implies that the quotient of these expressions will be the same for all i. This will be our verification step for both the matching of angles and the solution point obtained from an iteration. We must continue to match the smallest difference between the β-angles with the next smallest difference in the α-angles, and try all four iteration schemes in each case until the verification test passes. In the worst case $4n$ iteration schemes need to be tried.

5.1. An Example

We have used the algorithm described in Section 5 to recover slant and tilt of a number of model patterns. We have chosen one of these as a representative and report on this experiment in some detail here. The actual pattern in the object plane and the line segments that generate the β-angles are shown in Fig. 8. Because all angles between lines are approximately equal, this example is among the more difficult patterns to match. In any event, our method works on any point pattern, regardless of symmetries or other structural features of the pattern.

In the extreme case in which the object plane is parallel to the image plane the image will show a pure rotation of the pattern. The magnitude of the rotation is given by $\nu + \tau$, which equals $\alpha_i - \beta_i$ for any i, as immediately follows from Eq. (5.2) after substitution of $\cos\sigma = 1$. Evidently, the angles ν and τ can not be determined separately, and the iteration cannot converge in this case. It follows that for small slants very slow convergence should be expected. To handle small slants while avoiding extremely lengthy iteration sequences, the following can be done. Recall that when $\cos\sigma \approx 1$ the transformation is almost linear. Conversely, when we discover an almost linear relation between the two sets of angles we may conclude that the slant is small. We can then use this linear property to derive the approximation

$$\cos\sigma \approx \frac{\beta_{i+1} - \beta_i}{\alpha_{i+1} - \alpha_i} \tag{5.8}$$

from Eq. (5.2). The set (α_i, β_i) is assumed to be correctly matched and the result will be most accurate if i is chosen such that β_{i+1} and β_i straddle the x'-axis (because the projective effect is most strongly felt near the normal direction). These angles are easily recognized because a small gap is formed between β_i and β_{i+1} (as shown in Section 5) and the linear property will hold least for this particular pair. Thus the two sets of angles are first checked for a linear relation. If they are nearly linearly related, an approximate slant is calculated using Eq. (5.8). We will still try to iterate, but only for one candidate match. The justification is that when the transformation is almost linear the first match will generally be correct. If the iteration fails (because it has not converged within a fixed number of steps), the program will not waste time trying any other possible matches.

Accuracy of the solution depends on the termination criterion of the iteration process. We terminated when the difference between consecutive iteration values was less than 10^{-4}. The slower the convergence the less accurate the result will be. There is also an upper bound on the number of iterations in one sequence. We generally abandoned an iteration sequence if no sufficient convergence was reached after 150 steps. This number was raised to 300 steps in the case of an almost linear transformation.

The results are shown in Table 4 for increasing σ and an arbitrarily chosen tilt for each slant. The actual slant and tilt were known in this experiment and are listed in the first two columns. Columns 3 and 4 contain the calculated slant and tilt. No convergence was reached (within the bound limit) when $\sigma = 10°$. Column 5 shows the approximated slant values in those cases where an almost linear transformation was detected. Column 6 lists the total number of iterations required for those cases which terminated successfully. This number depends of course on the initial values chosen and is only shown to give a rough impression. We always started each iteration from $\tau = 0$ and $\nu = 0$. Column 6 shows the number of matches between the α's and β's that were tested before the correct correspondence was found. The last column shows the execution times (in seconds) on a VAX 11/750.

actual slant	actual tilt	calculated slant	calculated tilt	linear approx. slant	no. of iterations	no. of matches	time (in secs)
10	15	-	-	9.63	-	-	22
20	25	19.90	24.85	19.95	159	1	9
30	-65	29.97	-65.09	26.98	96	1	8
40	0	40.02	0.01	-	29	2	14
50	10	49.97	10.15	-	100	5	44
60	-15	60.00	-15.02	-	46	1	4
70	85	69.98	85.00	-	37	7	53
80	-20	80.01	-20.00	-	55	6	40
85	30	85.00	30.00	-	32	1	4

Table 4. Results for nine different orientations of the point pattern in Fig. 8.

6. Concluding Remarks

We have developed an iterative matching procedure for computing shape from contour using known planar models such as rectangles and point patterns. There are no restrictions on the types of polygonal contours or point sets which can be used with this technique. In most of our experimental results using point patterns, convergence was obtained very rapidly using four randomly selected pairs of points and our match heuristics for ordering the pairings of α- and β-angles.

Extensions of our technique can easily be defined for modeling each face of a three-dimensional planar-faced object. It remains to be investigated how multiple models can be efficiently used with images containing multiple objects. Another possible extension of interest is a study of the robustness of the procedure under distortions in either the model or image data. We found in the shape from rectangle experiments that if the actual ratio of sides was only approximately equal to the modeled value, convergence was still obtained in many cases with corresponding inaccuracies in the resulting surface orientation. The conditions under which solution accuracy can be traded off for solution speed (i.e. number of iterations) is also an open question. Future research includes studying this type of problem and developing methods for dealing with noisy data and images containing multiple, partially-occluded objects.

References

1. Kanade, T., Recovery of the three-dimensional shape of an object from a single view, *Artificial Intelligence* **17** (1981) 409-460.
2. Witkin, A. P., Recovering surface shape and orientation from texture, *Artificial Intelligence* **17** (1981) 17-47.
3. Brady, M. and Yuille, A., An extremum principle for shape from contour, *IEEE Trans. Pattern Analysis and Machine Intelligence* **6** (1984) 288-301.
4. Gregory, R. L., *Eye and Brain*, second edition, (McGraw-Hill, New York, 1973).

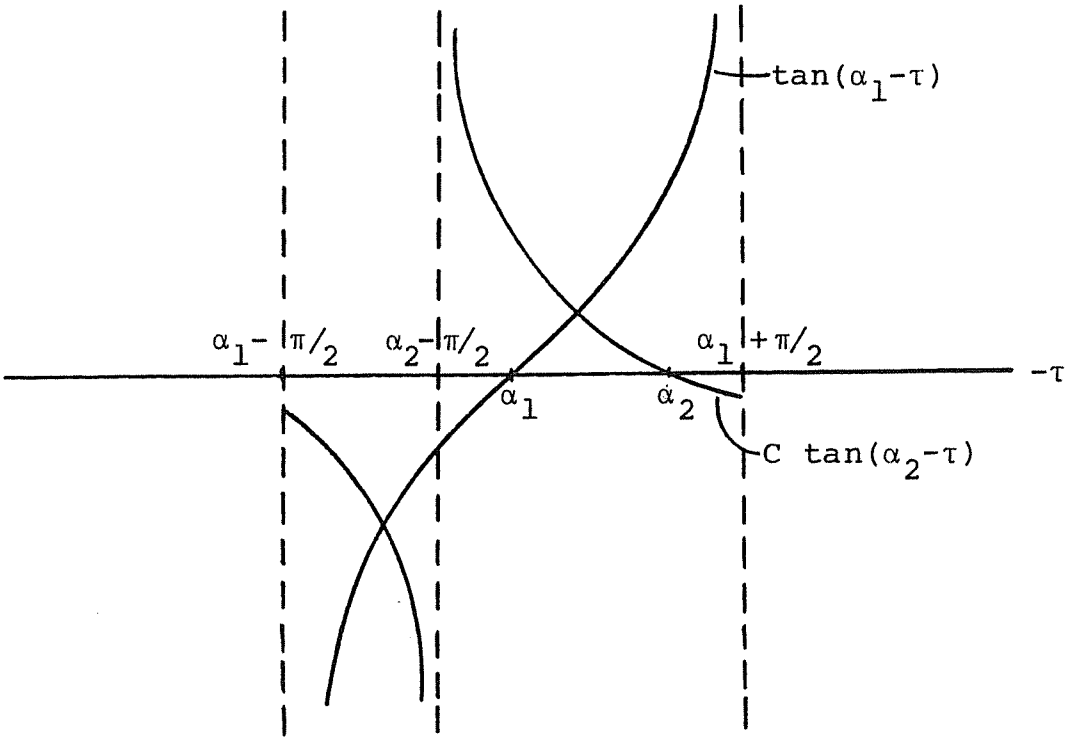

Fig. 1. (a) The two intersections of the tangent curves when $C<0$.

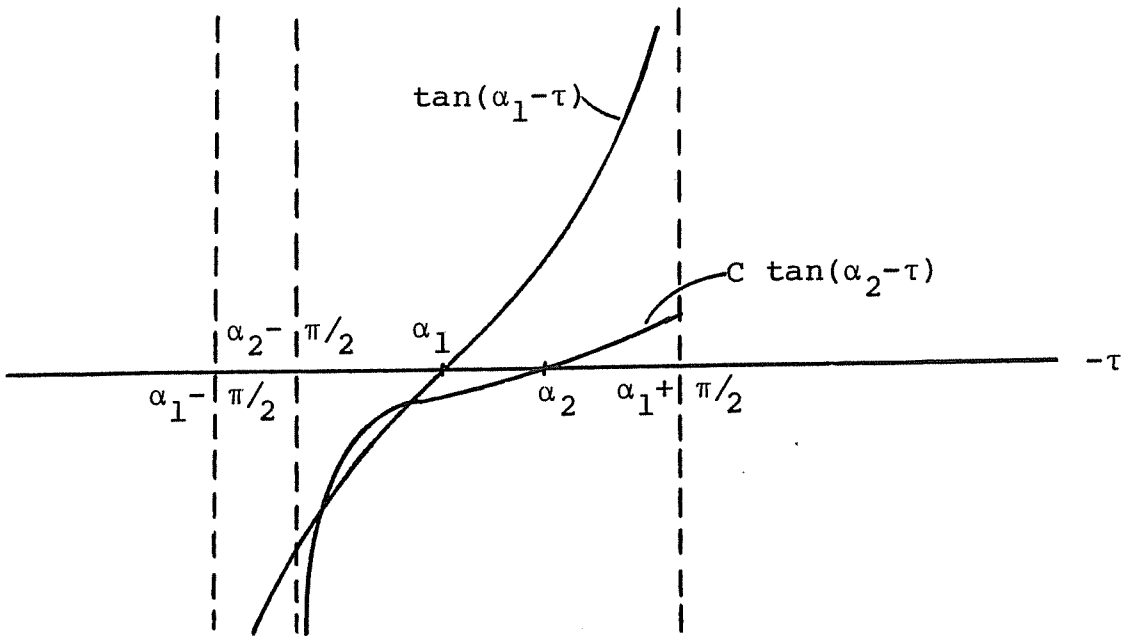

Fig. 1. (b) The two intersections of the tangent curves when $0<C<1$.

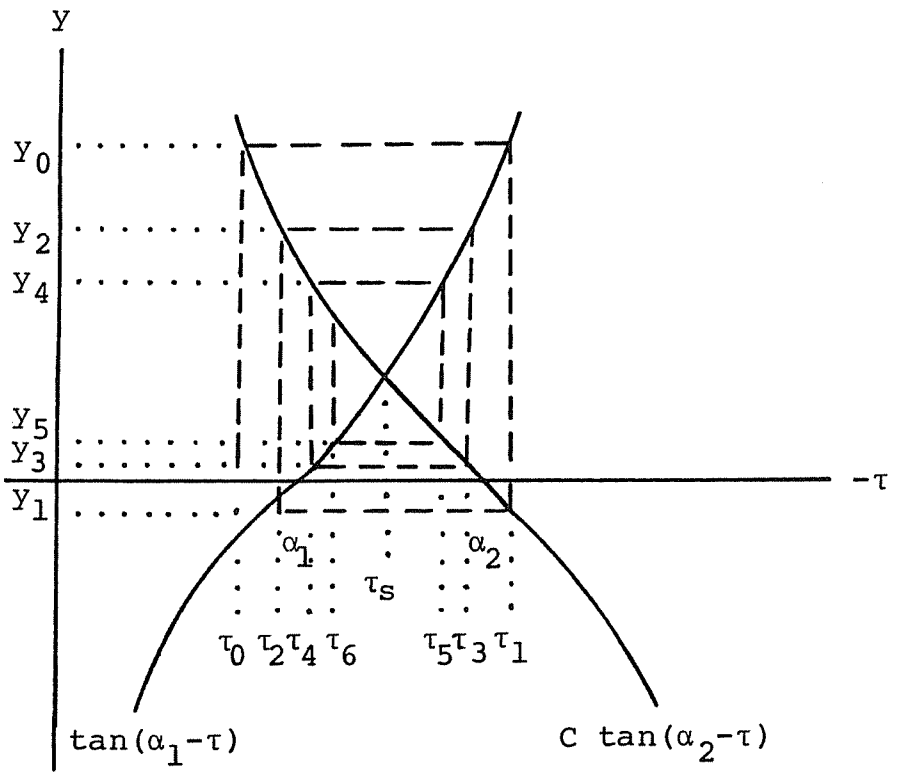

Fig. 2. (a) An inward-directed spiral for the case $C<0$.

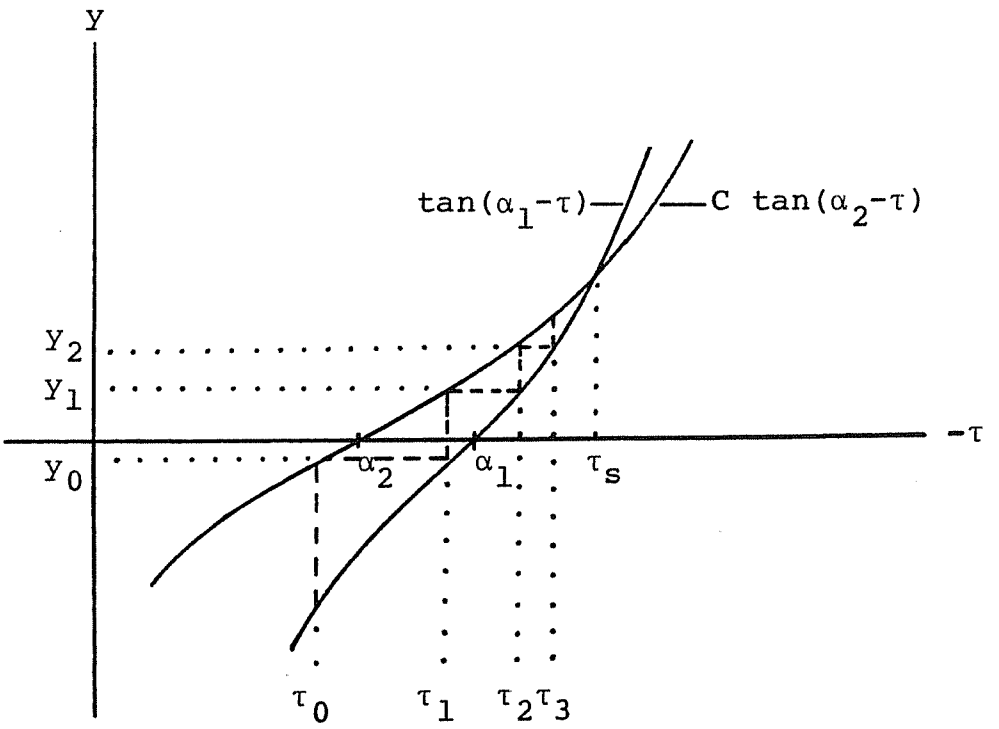

Fig. 2. (b) An inward-directed staircase for the case $C>0$.

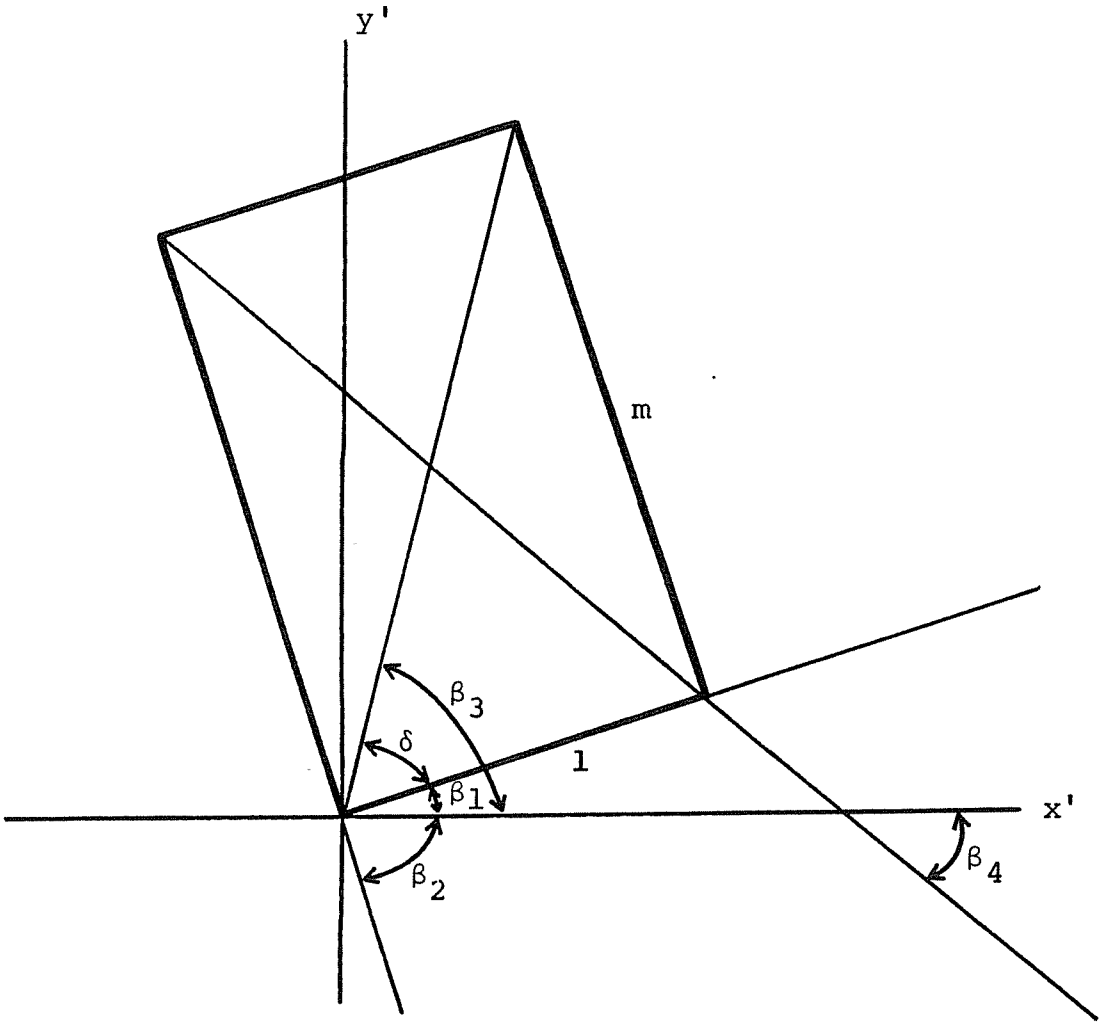

Fig. 3. The assignment of angles specifying a rectangle in the object plane S. The ratio of the sides is such that $\tan \delta = m$.

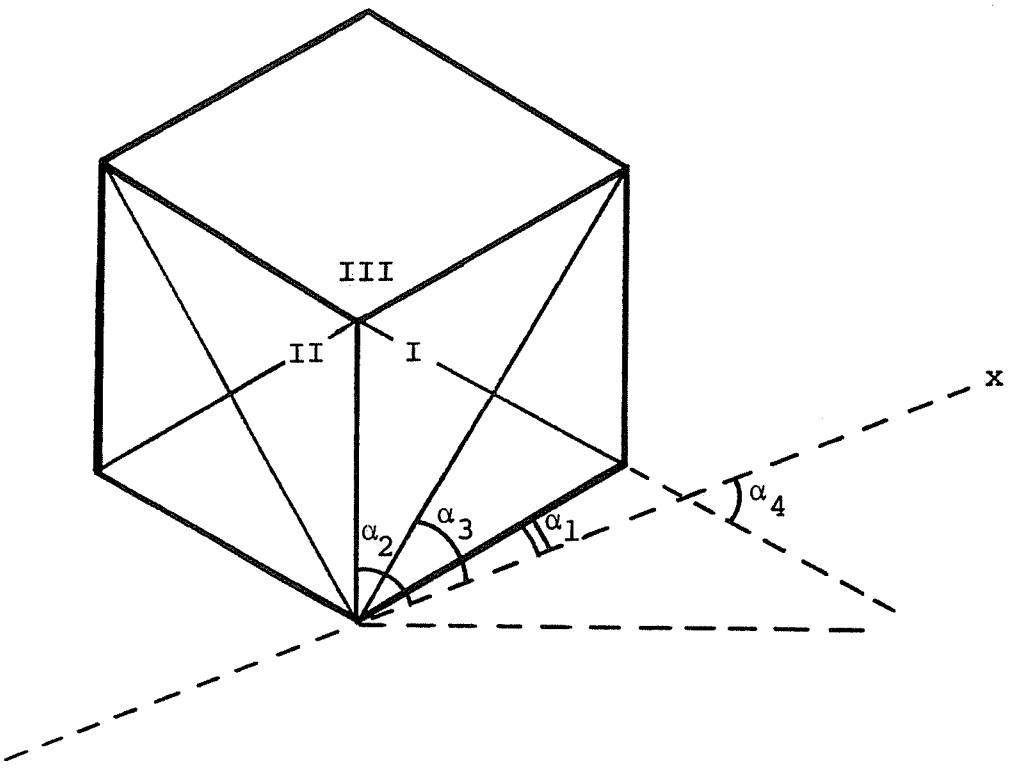

Fig. 4. The labeling of the three visible faces of a cube. The α-set shown is for face I.

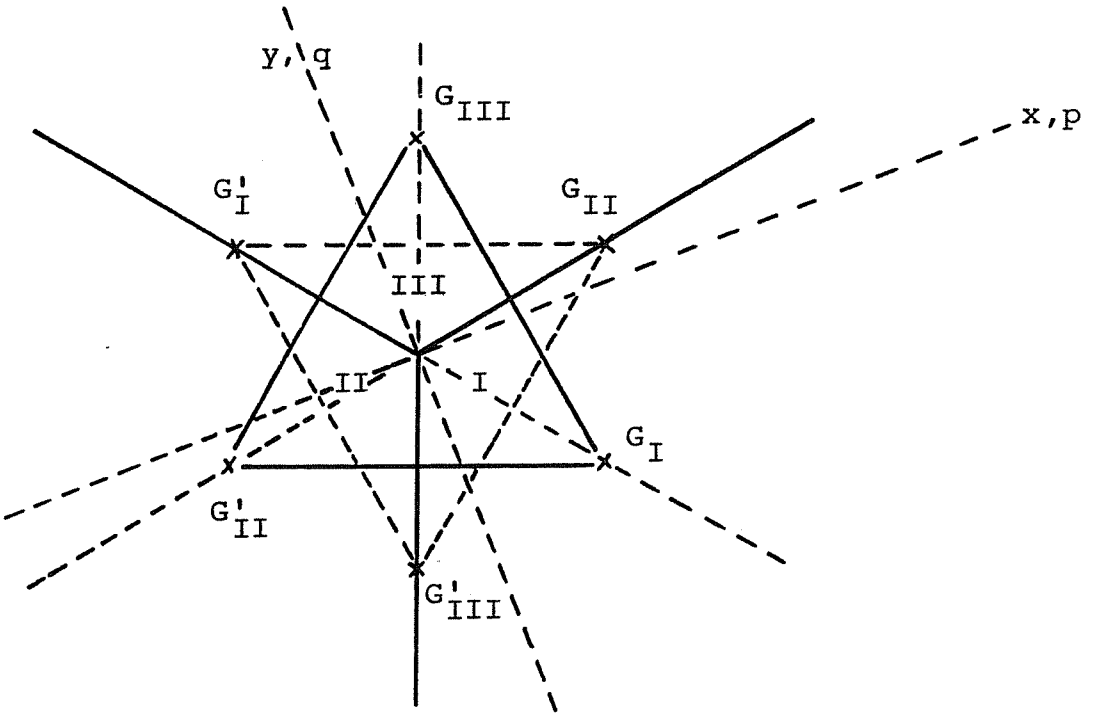

Fig. 5. Gradient space (p, q) superimposed onto coordinate space (x, y). Shown are the three faces of the cube and their two possible projected gradient directions. G_I, $G_{II}^{'}$ and G_{III} define the convex corner. $G_I^{'}$,G_{II} and $G_{III}^{'}$ define the concave corner.

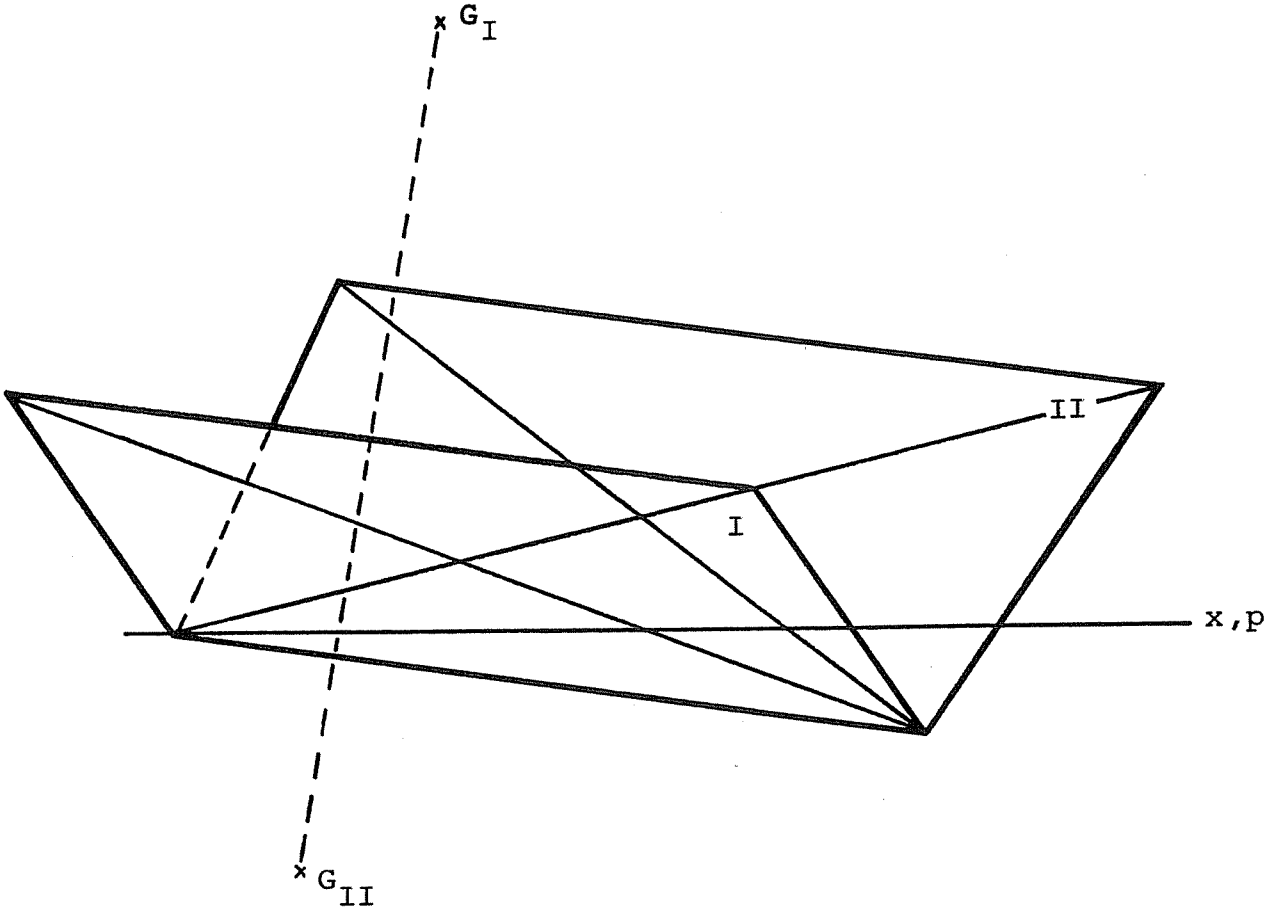

Fig. 6. A square piece of paper folded in the middle. Gradient space is superimposed on the image and the points G_I and G_{II} corresponding to the gradients of the two folds of paper are shown. The line connecting the gradient points is approximately perpendicular to the fold line.

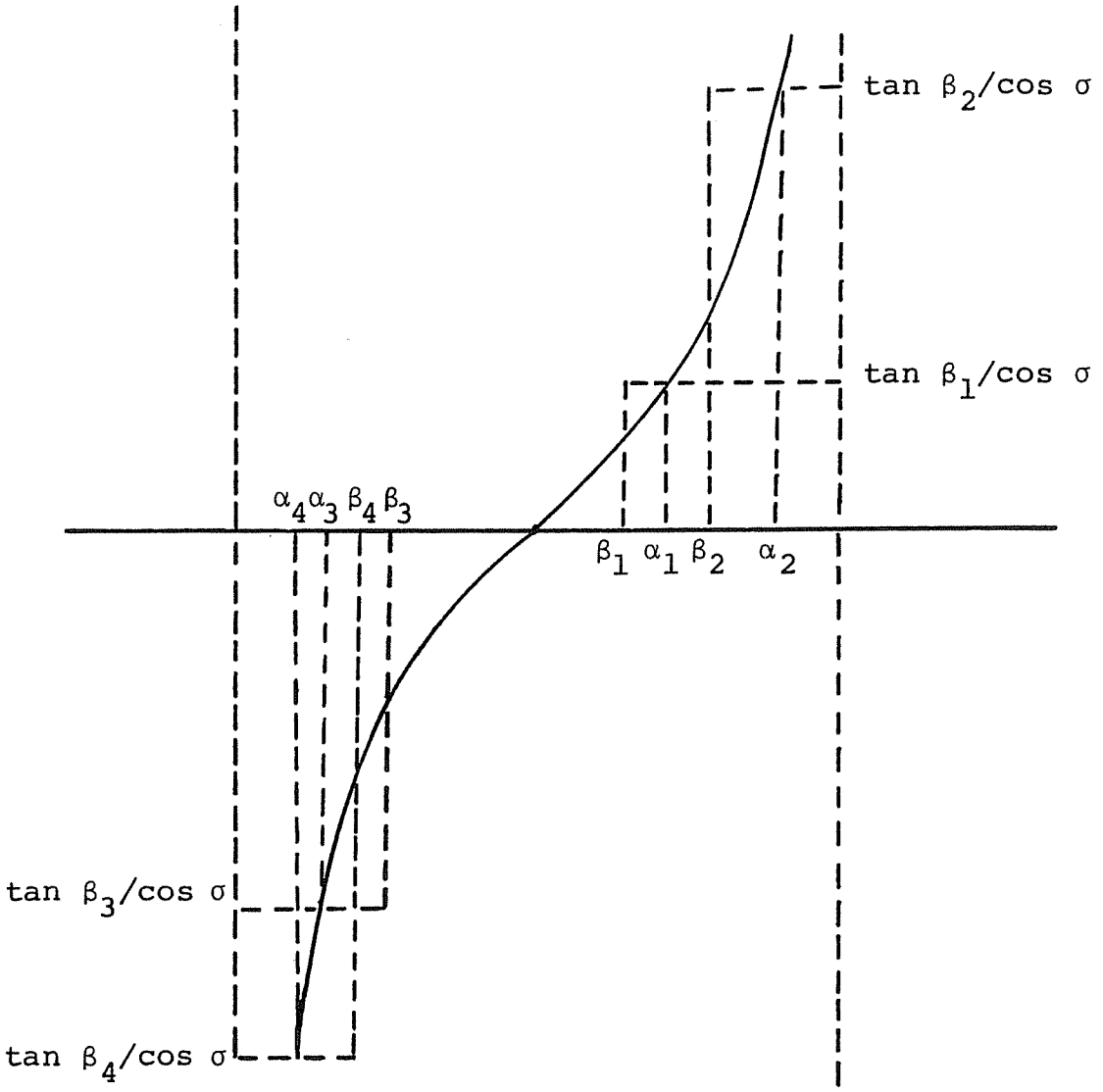

Fig. 7. The transformation $\beta_i \to \alpha_i$ as given by Eq. (5.7).

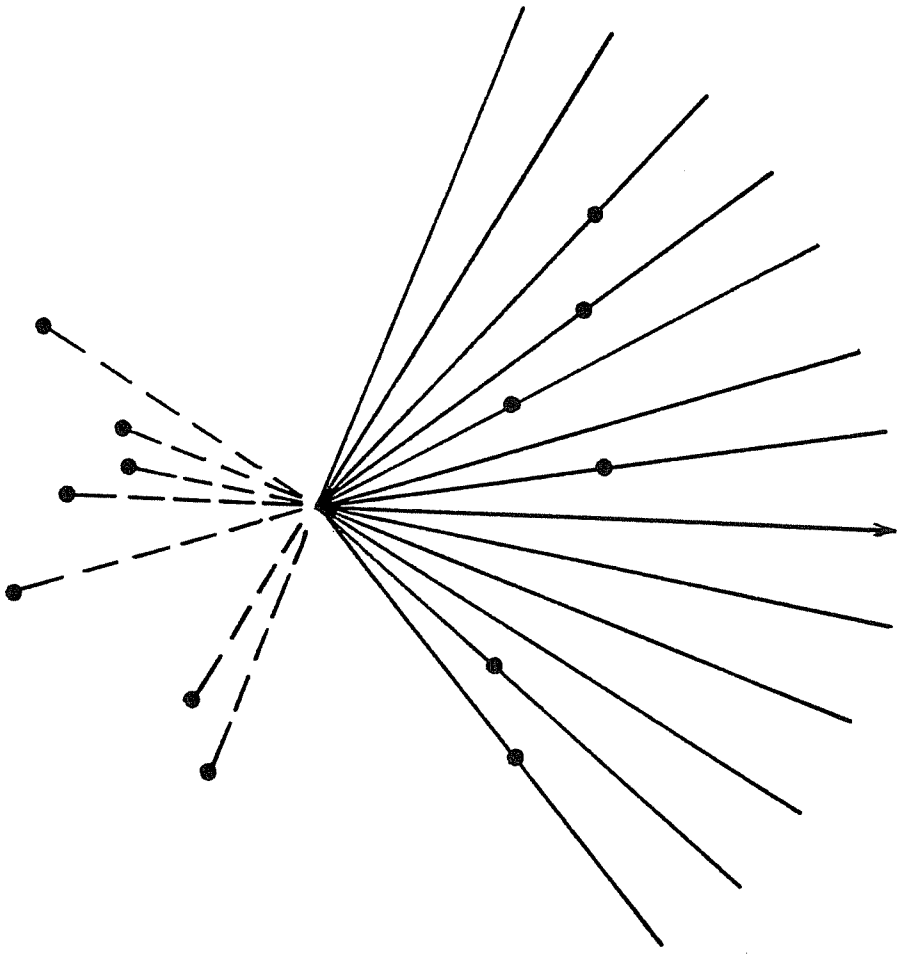

Fig. 8. A point pattern in the object space plane with the corresponding line segments generating the set of β-angles.